STUDIES OF SELECTED VOIDS. SURFACE PHOTOMETRY OF FAINT GALAXIES IN THE DIRECTION OF 1600+18 IN HERCULES VOID

G.Petrov [1] , A.Y.Kniazev [2] , and J.W. Fried [2]

[1] *Institute of Astronomy, Bulgarian Academy of Sciences, 72 Tsarigradsko chaussee, 1784 Sofia, Bulgaria;*
[2] *Max Plank Institut for Astronomy, Koenigstuhl 17, D 69117 Heidelberg, Germany*

Abstract: Based on photographic plates obtained with 2m RCC telescope at National Astronomical Observatory Rozhen (Bulgaria) we inspected an area of ~1 sq.degree in the direction of the Hercules void with automatic object detection software. As our first result we present a list of ~1800 detected galaxies in the wide range of magnitudes $13^m \leq B \leq 21^m$ and effective surface brightnesses $16 \leq \mu_{eff}(B) \leq 24$ mag arcsec^{-2}.

Introduction

The presence of voids in the distribution of galaxies has been discovered in early redshift surveys of galaxies - see e.g. [1, 2]. Further studies show that the largest voids are those delineated by rich clusters and superclusters of galaxies [3, 4]. The Hercules region has attracted the attention of astronomers since [5] discovered the Hercules supercluster covers a large area of the sky north of celestial equator in the range ascension range between $12^h < \alpha < 18^h$. A collaboration project between the Institute of Astronomy of Bulgarian Academy of Sciences and Max Plank Institute for Astronomy (Heidelberg, Germany) is devoted to investigate some known voids [6]. We present here the first results of a study of faint galaxies in the direction of Hercules void.

Observations

The observations were done during the nights of 27 and 28 June 1991. The Ritchie camera of the 2m RCC telescope at National Astronomical Observatory ″Rozhen″ (Bulgaria) was used to get two plates centered on RA(2000): $16^h01^m58^s$ and DEC: $+17°57′30″$ (No.1830 hereafter) and RA: $16^h02^m15^s$ and DEC: $++17°51′34″$ (No.1831 hereafter). The unvignetted field is ~50 sq.arc minutes for each plate and the common unvignetted field is ~1x1 sq.deg. The exposure time for each plate was 180

minutes, enough to detect objects fainter than 21 mag. Neutral wedge was exposed for 40 minutes on each plate after the main exposure. The seeing during the observations was very stable and varied only in the range of 1-1.5″. ORWO plate ZU21 30x30 sq.cm and Schott filter GG 385 were used to realize the standard B-system. To calibrate these data CCD frames in B and R were taken with 1024 x 1024 Photometrics camera, attached to the prime focus on the 2m RCC telescope during the night on July 28th 2003. M92 standard fields were observed twice during the same night.

Reduction

The two plates were scanned in the former Astronomical Institute, University of Muenster on PDS 2020 GMplus scanning machine with 25x25 mkm square slit and 20 mkm step, getting
14400 x 14400 sq.px with scale 0.25 ″/pixel. The linearization of the images was performed
with the photometer wedge and the program INTENAIP from the Astrophysical Institute of Potsdam (AIP) package [7, 8] added to the ESO MIDAS package.

We used a package of automatic procedures described in detail in [9] to detect objects above the background, to reject false detections, and to produce astrometry and integrated and surface photometry of detected galaxies. This software was created to work with Sloan Digital Sky Survey [10] data and was fitted for our purpose. The output data consist of a MIDAS table that contains all information about the detected galaxies: accurate positions (plate, X, Y, α(2000), δ(2000)), total and integrated magnitudes with their uncertainties, effective radii (R_{eff}; in arcsec), effective surface brightnesses (μ_{eff}; in mag arcsec^{-2}), radii of the regions containing 90% of the integrated (R_{90} ; in arcsec), concentration indices C=R_{90}/R_{eff} , position angle (PA), axial ratio (b/a), exponential fit scale lengths (α; in arcsec) with their uncertainties (in arcsec) for bulge and disk components, exponential fit central surface brightnesses ($\mu_{E;0}$; in mag arcsec^{-2}) with their uncertainties for bulge and disk components and total magnitudes, integrated out to infinity.
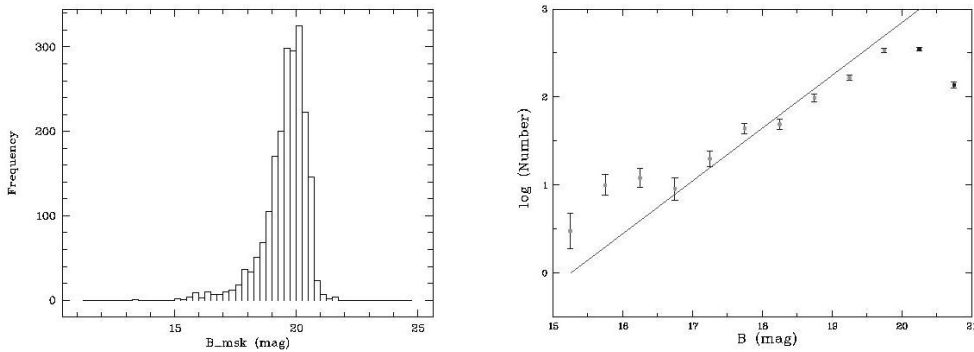
Figure 1: Left panel: Distribution of apparent magnitudes for all galaxies detected with

our programs. Right panel: Number counts of all galaxies detected with our programs as a

function of apparent magnitude. The errors bars on the galaxy counts are Poissonian. The

line shows the count-magnitude relation expected for a homogeneous galaxy distribution

in a universe with "Euclidean" geometry: $N(B) = A_B . 10^{0.6B}$.

Integrated photometry: A code for fitting the sky background from the AIP package for adaptive filtering is used, which constructs the background within the masked regions. This algorithm iteratively fills the background inside the mask by interpolating the background from the regions outside the mask [7, 8] and it is used twice: 1) to subtract any contaminating sources like foreground stars or background galaxies and 2) to fit and subtract the sky background. During the next step we iteratively checked all detected objects by eye to identify multiple and false objects. After that the apparent is measured inside the same mask on the background-subtracted images. The instrumental is transformed into the apparent magnitude in the standard photometric system (see Fig.1). Firstly, we used the NED magnitudes for the bright galaxies in the our field to calibrate the data and finally we got M92 calibration frames (see above).
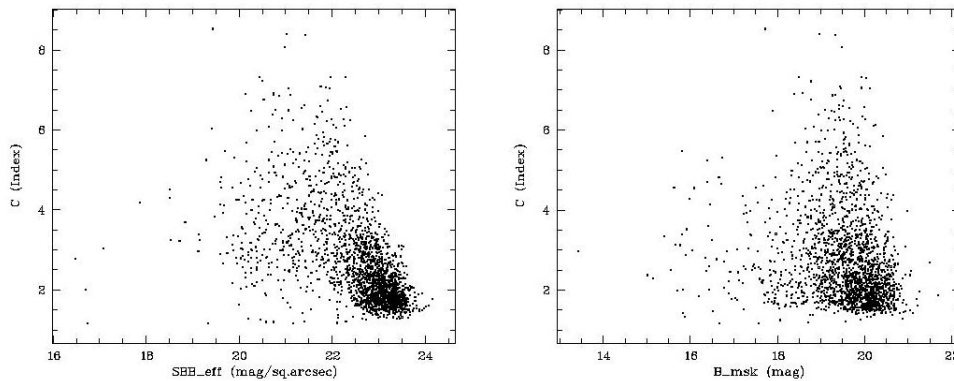
Figure 2: Relations between the concentration index and effective surface brightness (left panel) and the integrated magnitude (right panel).

Morphological types and concentration index: Our programs calculate a number of global parameters for every galaxy. Some of these may be useful for morphological galaxy classifications [11]. A particularly useful parameter is the concentration index, defined as the ratio of the radii containing 90% and 50% of a galaxy's light. For the classical de Vaucouleurs profile C is ~5.5 and for pure exponential disks C~2.3. These values are valid for the idealized seeing-free case (see Fig.2).

Creation of surface brightness profiles (SBP): The software generates SBP by measuring magnitudes in circular apertures. After a SBP is created, the effective radius R_{eff}, R_{90} and the concentration index C are calculated. Using the multilevel mask approach and ellipse fitting we also determine the PA of the major axis and the axis ratio *b/a*.

First Results

The data for all 1814 galaxies in the field - coordinates, aperture and surface photometry,
position angles, diameters, axis ratio and concentration are available under question or on- line in FITS format at
http://www.astro.bas.bg/~petrov/papers/hercules/v16t1.fits.

Giant Low Surface Brightness galaxies (LSBG): An interesting aspect of this pilot study is the identification of a substantial number of luminous distant galaxies. In Fig.3 the relations between the concentration index and the effective surface brightnesses μ_{eff} and the integrated magnitude are plotted. Some LSBGs could be selected there - bright

galaxies with B~15.5-18 mag or such ones with large diameters (> 40 arcsec) and SB > 22 mag/sqr.sec.

Galaxy Number Counts: The number counts of galaxies as a function of magnitude is one of the classical cosmological tests. We did it for our data and the result is plotted on the right panel of Fig.1. Galaxy number counts are shown in 0.5 mag bins. The errors bars correspond to
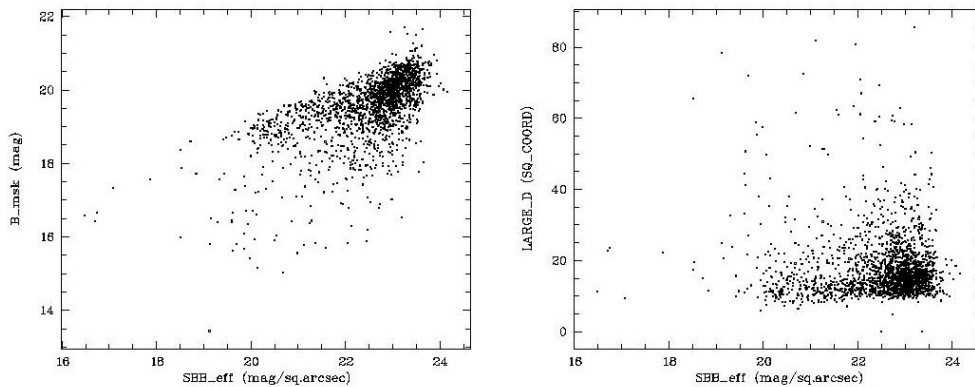

Figure 3: Left panel: Relation between the effective surface brightnesses and integrated
magnitude. Right panel: Relation between the effective surface brightnesses and major diameter of galaxies.

Poisson noise. The line in Fig.1 shows a fit to the galaxy counts-magnitude relation expected in a homogeneous universe assuming Euclidean geometry for three-dimensional space. The observed galaxy counts are quite consistent with this line for $17^m \leq B \leq 20^m$ and even fainter up to B=20.5 mag. It means that we have complete data up to this magnitudes. With our data we found big excess of bright galaxies (B<17.0^m).

References

[1] C h i n c a r i n i, G. & H.J. R o o d. The cosmic tapestry, Sky and Telescope, 59,1980,364

[2] G r e g o r y, S.A. & L.A. T h o m p s o n. Superclusters and voids in the distribution of galaxies, Sci. Am., 246, 1982, 106

[3] O o r t, J. Superclusters, Ann.Rev.A&Ap., 21, 1983, 373

[4] R o o d, H.J. Voids, Ann.Rev.A&Ap., 26, 1988, 631

[5] S h a p l e y, H. On some structural features of the metagalaxy, MNRAS, 94, 1934, 791

[6] P e t r o v, G., B. K o v a c h e v, & A. S t r i g a t c h e v. A search for galaxies in voids – first results, Astron.Ges. Abstr.Ser., 9, 1993, 46

[7] L o r e n z, H., G.M. R i c h t e r, M. C a p a c c i o l i, & G. L o n g o. Adaptive Filtering in Astronomical Image Processing – P1- Basic Considerations and Examples, A&A, 277, 1993,321

[8] K n i a z e v, A.Y. Ph.D. Thesis, Special Astrophys. Obs., Nizhnij Arkhyz, 1997

[9] K n i a z e v, A.Y., E.K. G r e b e l, S.A. P u s t i l n i k, A.G. P r a m s k i j, T.F. K n i a z e v a, F. P r a d a & D. H a r b e c k. Low-Surace-Brightness Galaxies in the Sloan digital sky survey. I. Search method and test sample, AJ, 127, 2004, 704

[10] Y o r k, D.G., J. A d e l m a n, J.E. A n d e r s o n et al. The Sloan Digital Sky Survey: Technical Summary, AJ, 120, 2000, 1579

[11] S t r a t e v a, I., Z. I v e z i c, G.R. K n a p p et al. Color Separation of Galaxy Types in the Sloan Digital Sky Survey Imaging Data, AJ, 122, 2001, 1861